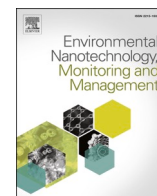




Contents lists available at ScienceDirect

Environmental Nanotechnology, Monitoring & Management

journal homepage: www.elsevier.com/locate/enmm

Mycogenic fabrication of silver nanoparticles using *Picoa*, Pezizales, characterization and their antifungal activity

Mustafa Nadhim Owaid^{a,b,*}, Muwafaq Ayesh Rabeea^c, Azlan Abdul Aziz^d,
Mahmood S. Jameel^d, Mohammed Ali Dheyab^d

^a Department of Heet Education, General Directorate of Education in Anbar, Ministry of Education, Hit 31007, Anbar, Iraq

^b Department of Environmental Sciences, College of Applied Sciences-Hit, University Of Anbar, Hit 31007, Anbar, Iraq

^c Department of Applied Chemistry, College of Applied Sciences-Hit, University Of Anbar, Hit 31007, Anbar, Iraq

^d Nano-Optoelectronics Research and Technology Lab (NORLab), School of Physics, Universiti Sains Malaysia, 11800 Pulau Pinang, Malaysia

ARTICLE INFO

Keywords:

Antifungal activity
AgNPs
Biosynthesis
Desert truffles
Plant-pathogenic fungi

ABSTRACT

In this work, silver nanoparticles have been mycofabricated from *Picoa* sp. (a desert truffle) for the first time. Also, the antifungal activity of *Picoa*-AgNPs has been investigated against three pathogenic fungi, including *Pythium* sp., *Aspergillus flavus*, and *Aspergillus niger*, which can cause severe damage to health and agriculture. Morphology and physico-chemical characteristics of the mycofabricated AgNPs were thoroughly described by UV-VIS, XRD, FESEM, TEM, FT-IR and Zeta Potential analyses. The optimum synthesis time of the AgNPs during the reaction progress was 60 min and outstanding at the peak of 440 nm. Nano-irregular shapes with an average size of 19.5 nm and high stability (-20.9 mV) have been recorded. FT-IR spectra showed high amino acid content in the *Picoa* sp. extract efficiently will achieves the bioreduction reaction of Ag ions to Ag atoms. The higher inhibition percentage of *Picoa*-AgNPs was 30.81% against *Pythium* sp. at the concentration of 10%, while the concentration of 5% showed a low inhibitory effect (13.51%). The concentration of 5% exhibited an inhibitory impact reached 16.67% against *Aspergillus niger*. These findings have shown a promising outlook for the use of *Picoa* (Pezizales) in the production of AgNPs for its use as antifungal nanodrug.

1. Introduction

Nanotechnology is a remarkable process changing properties of materials, such as the scale, distribution and shape of particles, which have tremendous possibilities for use in human life (Roseline et al., 2019). The used chemicals in the preparation of nanomaterials attract toxins that mobilize to the surrounding environment. In the last few decades, remarkable efforts have been made to continue making nano-material production in the green routes to decrease the toxicity toward humans, animals and plants (Bhattarai et al., 2018). Many studies reported that the green method used to synthesize AgNPs inhibited plant pathogens (Gopinath and Velusamy, 2013) like bacteria and fungi species (Owaid, 2020). As desert truffles are high in protein, amino acids are considered reducing agents to reduce silver ions to Ag atoms in the form AgNPs (Khadri et al., 2017; Owaid, 2018). The green synthesis of silver nanomaterials achieved by the mushroom (Owaid, 2019c), or truffles, including *Pleurotus cornucopiae* (Owaid et al., 2015), *Inonotus hispidus* (Jaloot et al., 2020), *Agaricus bisporus* (Owaid et al., 2020),

Ganoderma applanatum (Jogaiah et al., 2019), *Coprinus comatus* (Naeem et al., 2021), and *Tirminia* sp. (Owaid et al., 2018). Also some molds (*Trichoderma harzianum*) and (Konappa et al., 2021) medicinal plants (*Dillenia indica*) (Nayak et al., 2020) were used to produce green AgNPs. Due to their excellent physical and chemical characteristics, silver nanoparticles have been applied in a wide range of important scientific fields like antibacterial (Owaid et al., 2018), antifungal (Jaloot et al., 2020), anticancer (Owaid et al., 2020), antioxidant activities (Ahn et al., 2019) and catalytic degradation of Azo dyes (Khandan Nasab et al., 2020). However, there are many recent applications for green AgNPs in the medical field like the *Ganoderma applanatum*-AgNPs which were used to inhibit bacteria because of their high phenolic content (Jogaiah et al., 2019). The *Dillenia indica*-AgNPs was used to inhibit different pathogenic bacteria such as *Enterococcus faecalis* and *Escherichia coli* (Nayak et al., 2020). The *Trichoderma harzianum*-AgNPs were applied as nanodrugs against *Staphylococcus aureus*, *Bacillus subtilis*, *E. coli* and *Ralstonia solanacearum* (Konappa et al., 2021).

Antifungal nano agents differ from classical antifungals (Gherbaw

* Corresponding author.

E-mail address: mustafanowaid@uoanbar.edu.iq (M.N. Owaid).

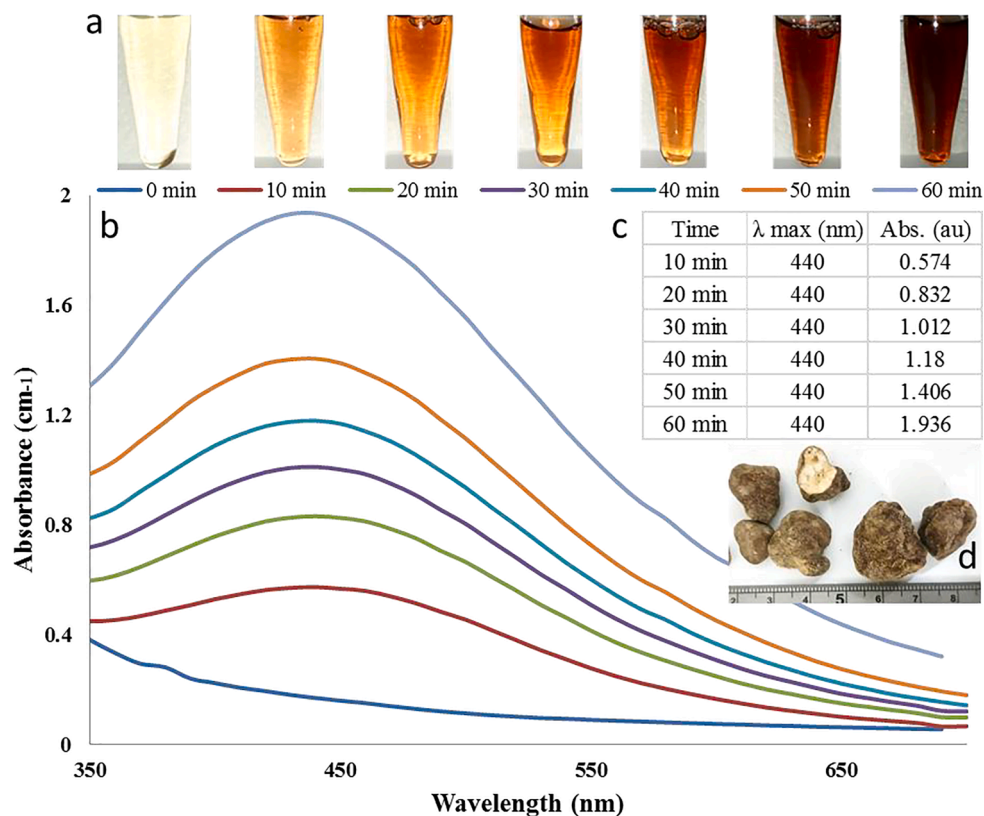


Fig. 1. Optical vision and UV-Vis spectra of the mycosynthesized AgNPs. Legend: (a): The color of colloidal AgNPs with increasing time of interaction, (b): UV-Vis spectra from 350 to 700 nm, (c): The Lambda max for each time, and (d): Ascocarps of *Picoa* sp.

et al., 2013). At the same time, nanomaterials are similar to most biological molecules and can be diffused across cell membranes because of their fine sizes (Gupta et al., 2018). Thus, this feature encouraged to use green nanoparticles in the health and agriculture field, especially against fungal pathogens (Ismail et al., 2017; Purohit et al., 2019).

Desert truffles are a source of essential nutrients and the most expensive food; they are common in Asia and Europe (Wang and Marcone, 2011). Antibacterial and antioxidant activity of desert truffles has been reported and used for medicinal purposes (Chen et al., 2016). *Picoa* sp. is one of the desert truffles belonging to Pezizales, and it is known in the arid and semi-arid regions of the Middle East and Mediterranean areas (Owaid, 2018). Its fruiting bodies contain more than 20 amino acids and more than 10 fatty acids. They also contain 23% carbohydrates, and 18% fibers, (Bawadekji et al., 2016; Martínez-Tomé et al., 2014).

Even though extracts of many species of fungi have been recently used for the preparation of metallic nanoparticles (Abdul-Hadi et al., 2020; Dheyab et al., 2020; Eskandari-Nojehdehi et al., 2018; Eskandari-Nojehdehi et al., 2016; Owaid et al., 2019, 2018; Rabeea et al., 2020), *Picoa* sp. has never been used as a reducer to mycosynthesize silver NPs. Here, the first attempt to fabricate of silver NPs using *Picoa* ascocarps reports from their aqueous extract. The synthesized *Picoa*-AgNPs have been diagnosed by some analytical techniques to explain their morphological, structural, and chemical properties. Furthermore, the antifungal activity of those AgNPs was investigated.

2. Materials and methods

2.1. Fungal samples

The ascocarps of *Picoa* sp. were collected from Anbar Desert and identified as *Picoa* according to morphological characteristics (Jamali and Banihashemi, 2013). These ascocarps were used for the

nanoparticles synthesis. Three plant pathogenic fungi were obtained from University of Baghdad (College of Agricultural Engineering Sciences) to do the antifungal activity of the biosynthesized silver nanoparticles (AgNPs). They are *Aspergillus niger*, *Aspergillus flavus* and *Pythium* sp.

2.2. Extraction of ascocarps

The hot extraction method was used to obtain the crude aqueous extract of *Picoa* sp. Seven grams of fresh *Picoa* sp. ascocarps was extracted in 50 ml DW (Distilled Water) under boiling for 10 min. The extract has been filtered, centrifuged at 4000 rpm for 15 min and the clear extract collected in a clean test tube for achieving this study, but the residue was stored at freeze for future studies.

2.3. Mycosynthesis of *Picoa*-silver nanoparticles

The green method was used to synthesis *Picoa*-AgNPs. After boiling 50 ml AgNO_3 10^{-1} M, 15 ml of *Picoa* extract was added with continuous stir on the hot plate magnetic stirrer. The temperature was decreased to 80 °C, and then 3 ml of the mixture was taken after 10, 20, 30, 40, 50, 60 min to check UV-Visible spectra and optical vision.

2.4. Characterization of *Picoa*-silver nanoparticles

The mycosynthesized AgNPs from *Picoa* sp. ascocarp extract were described using optical vision, FTIR (Fourier-transform infrared, Shimadzu, AV-1800) spectroscopy, UV-Visible spectrum (EMCLAB UV/VIS Spectrophotometer, Germany, Model EMC-11S-V, 325–1000 nm), TEM (Transmission Electron Microscopy), FESEM (Field-Emission Scanning Electron Microscopy, FESEM-FEI/Nova NanoSEM 450), XRD (X-Ray Diffraction, Bruker, Shimadzu, Japan), and Zeta Potential (Nanoseries Model ZEN 3600, Malvern Instruments) analyses. The average grain size

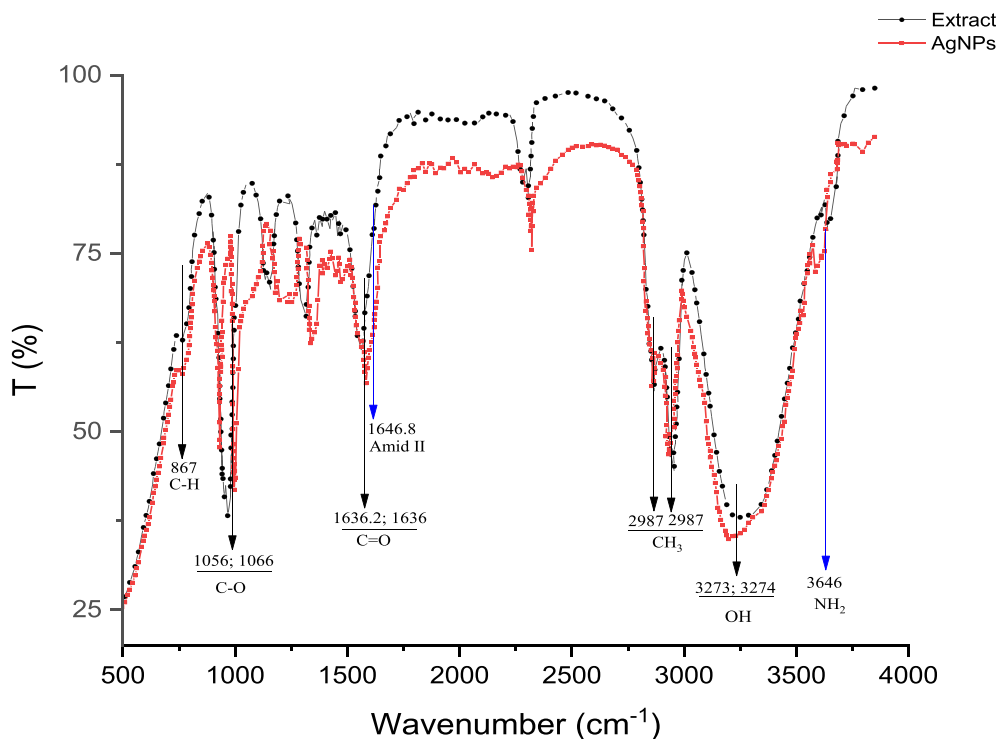


Fig. 2. FTIR of the extract of *Picoa* and the biosynthesized *Picoa*-AgNPs. Legend: (Extract): the extract of *Picoa*, and (AgNPs): the biosynthesized *Picoa*-AgNPs.

of the mycosynthesized AgNPs was determined using the diffraction peak of X-ray according to Debye–Scherrer equation (Abdelrahim et al., 2017). Some analyses were done at Universiti Sains Malaysia (USM), Malaysia.

2.5. Antifungal activity

The anti-fungal efficacy of the biosynthesized silver NPs and the mushroom extract alone have been done according to the well diffusion method (Owaid et al., 2017). Two concentrations of the extract (5% and 10%) and two concentrations of the biosynthesized AgNPs (5% and 10%) have been placed in fresh dishes in PDA (Potato Dextrose Agar) and left at 2–4 °C for half-hour until spreading the solutions in agar. The dishes have been inoculated by the discs of old 7-days fungi in their centres, incubated at 28 ± 1 °C to monitor and record the mycelial growth's diameters. The fungal isolates have been inoculated in plates without AgNPs or the mushroom extract as control. The inhibition percentage has been evaluated using Eq. (2) (Owaid, 2017):

$$\text{Inhibition Percentage} = [(I1 - I2)/I1] * 100 \quad (2)$$

where I1: the control dish diameter, I2: the treatment dish diameter.

2.6. Statistical analysis

In this study, the SAS software was used to design the experiment in CRD (Completely Randomized Design) using the influence of two factors (the concentration of *Picoa*-AgNPs or mushroom extract and species of pathogen). The statistical analysis has been done using one-way variance at $p < 0.05$ with triplicates.

3. Results and discussion

Picoa has moderate protein content, but it has never been used to reduce silver ions. As a result, in the current study, a greener method of *Picoa* aqueous extract has been used to aid in the fabrication of silver nanoparticles. The reaction's progress was monitored at 10, 20, 30, 40,

50 and 60 min to obtain the optimum preparation time for the synthesis of AgNPs. Interestingly, the reaction medium, which contained 50:5 (V/V ml) of 1 mM silver nitrate and *Picoa* extract, changed colour from bright yellow to brown after 10 min of stirring at 80 °C. This demonstrates a rapid nucleation of silver nanoparticles detected at 440 nm (Fig. 1). The activation process of the reduction for Ag^+ to a zero-valent state (Ag^0) is achieved by amino acid (released from *Picoa* sp.) accompanied by nucleation of the metal atom (Malik et al., 2014). These results agreed with the results of the desert truffle *Tirminia*-AgNPs colloids (Owaid et al., 2018) and many recent studies for mushroom-AgNPs (Al-Bahrani et al., 2017; Owaid et al., 2020, 2015) due to the Surface Plasmon Resonance (SPR) excitation in the medium of silver-NPs (Shankar et al., 2003).

FT-IR (Fourier-transform infrared) spectra have been used to characterize the aqueous extract of *Picoa* (Pezizales) and *Picoa*-AgNPs. Fig. 2 exhibits the *Picoa* spectrum indicating polysaccharide and protein are the main structure of the *Picoa* extract. The broad absorption peak at 3373.9 cm^{-1} assigned to the hydroxyl bond's stretching mode; another peak was located at 3349.57 cm^{-1} for NH_2 group in the protein. The closely spaced peaks at 2987.7 cm^{-1} and 2901 cm^{-1} are associated with "out of ethyl group stretching" and "in methyl group stretching" of fatty acids available in the protein, respectively. A strong absorption peak at 1636 cm^{-1} corresponded with the carbonyl group (C=O), and the stretching vibration peak at 1646.8 cm^{-1} suggested the existence of primary amid ($-\text{CO}-\text{NH}_2$) in the protein. The sharp absorption peaks between 1066 cm^{-1} and 1056 cm^{-1} defined the C-O group's expansion in the carbohydrate. Stretch peaks in the region between 1455.9 cm^{-1} and 1383 cm^{-1} are associated with the peptide bond functional groups in amino acids. Presence of two peaks at 1250.5 cm^{-1} and 1075.3 cm^{-1} in *Picoa* extract, due to alcohol (C-O) and (C-N) amine groups, respectively. The peak at 867 cm^{-1} referred to the vibration of the aromatic (C-H) group in the amino acid present over the protein molecule.

After the redox reaction between the silver ions and the aqueous extract, some of the major peaks repeated, and another disappeared. High protein content in *Picoa* extract reduced the Ag^{+2} that were confirmed in Fig. 2. This figure showed the two slight peaks assigned to

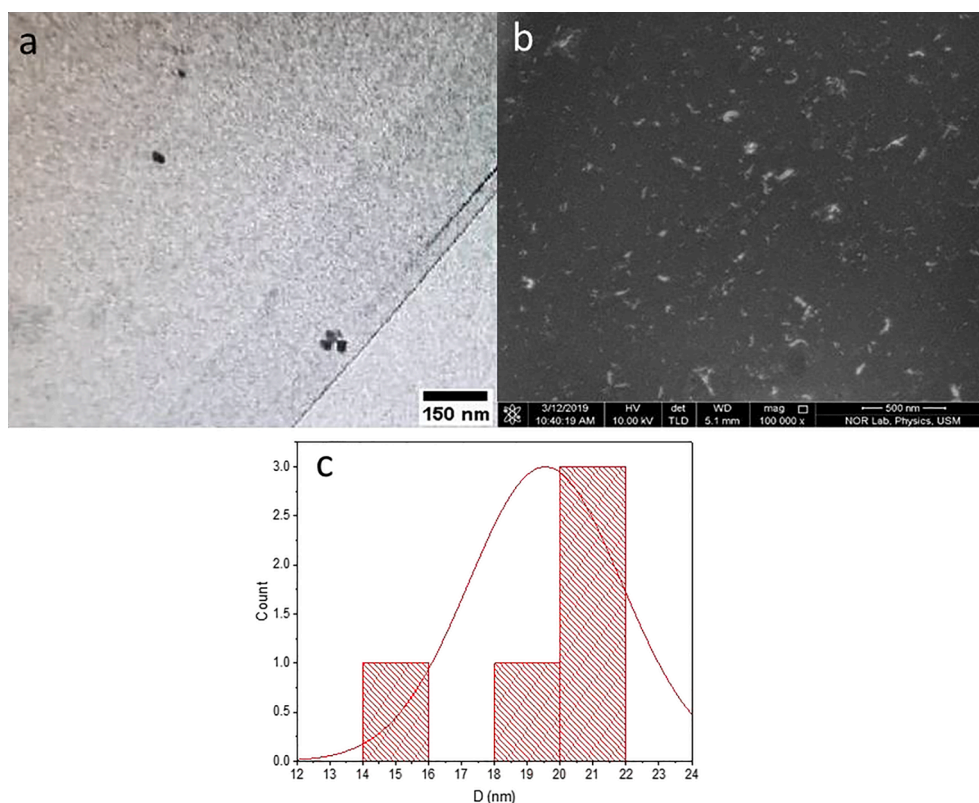


Fig. 3. Electron microscopic features of the mycosynthesized Picoa-AgNPs. Legend: (a): FESEM, (b): TEM, and (c): The histogram of the AgNPs.

Table 1

Microstructural parameters and sizes of the mycosynthesized AgNPs from *Picoa*.

Planes	Peak position 2θ ($^{\circ}$)	FWHM β size ($^{\circ}$)	d-spacing [Å]	The dislocation density ($\times 10^{15}$ lines/ m^2)	Diameters of crystals (nm)
(111)	38.0746	0.7872	2.36351	8.0292	11.16
(200)	44.2050	0.2952	2.04892	1.0849	30.36
(220)	64.7163	0.246	1.44044	2.3203	20.76

the functional amino group (3565.9 cm^{-1}) and the functional carboxyl group (1646.8 cm^{-1}). This clearly indicated their participant in the covalent bond among functional groups of the protein molecule and the carboxylic acid with new material (*Picoa*-Ag nanoparticles).

FESEM (Field-Emission Scanning Electron Microscopy) and TEM (Transmission Electron Microscopy) (Fig. 3) of the myco-synthesized silver NPs show the size and shape of NPs exhibited formation of irregular silver nanoparticles with an average ranging from 15 to 35 nm.

Table 1 showed results of XRD (X-Ray Diffraction) pattern for *Picoa*-AgNPs mycosynthesized by the watery crude extract of ascocarp of *Picoa*, indicated pure crystalline silver nature. Moreover, the reflection peaks exhibit formation of AgNPs with high purity, observed at 11.16 nm, 30.36 nm and, 20.76 nm, which correspond to (111), (200), and (220) planes, respectively.

The pattern of XRD was crystalline and showed Bragg's peaks, which indicated the structure of face-centred cubic (FCC) related to nanostructures of Ag. These nanostructures correlated well with standard peaks of Ag element as in the data card 04-0784 (JCPDS). Three peaks appeared, including (111), (200) and (220) planes. The broadening peaks and the properties of FCC nanostructure affirmed the mycosynthesizing AgNPs. The grain sizes (Diameter) of the mycosynthesized Ag NPs were 11.16 nm, 30.36 nm and, 20.76 nm for (111), (200), and (220) planes, respectively; while the average size of these crystals was 20.76 nm. To evaluate the average of the AgNPs size, the equation of

Debye-Scherrer Eq. (1) was employed (Owaid et al., 2020):

$$D = \frac{k\lambda}{\beta \cos\theta} \quad (1)$$

Whereas the dislocation density (δ) has been calculated by Eq. (2) (Abdul-Hadi et al., 2020):

$$\delta = (1/D^2)$$

where 'D' is the diameter of NPs (size), Lambda (λ) is the wavelength of X-ray (0.15406 nm), the constant K is approx. 0.89, Bragg angle (θ) is for the diffraction, β is the value of FWHM (Full Width Half Maximum). The microstructural parameters and nanoparticle sizes of the *Picoa*-AgNPs are listed in Table 1.

The stability of mycofabricated silver NPs has been done using measurement of zeta potential analysis as in Fig. 4. This analysis exhibited recording charges on the surface of AgNPs. Values of this analysis indicate the stability of mycosynthesized nanoparticles (Srikar et al., 2016). The mycofabricated AgNPs exhibited a good negative value for zeta potential of $-20.9 \pm 4.97 \text{ mV}$ prepared from the extract of *Picoa*. This result referred to finding aggregation of nanoparticles with good quality. The negative charges referred to that AgNPs are surrounded by negative biomolecules, which reduce repulsion among AgNPs, decrease the aggregation, and increase their stability (Suresh et al., 2011).

Many studies have referred to that biomolecules making as a surface-active stabilizer in the reaction mixture led to more stable AgNPs by creating electrostatic interactions (Irvani et al., 2014). However, some molds (*Trichoderma harzianum*), mushrooms (*Ganoderma applanatum*) (Jogaiah et al., 2019), and (Konappa et al., 2021) medicinal plants (*Dillenia indica*) (Nayak et al., 2020) were used to produce green AgNPs. It is suggested that organic molecules like protein, amino acid, and carbohydrate can act as surface-active molecules responsible for the mycosynthesis and stability of AgNPs. AgNPs are considered stable if their potential surface value ranges from -30 to $+30 \text{ mV}$ (Anand et al., 2015). Nevertheless, the stable dispersion of Ag nanoparticles is clear

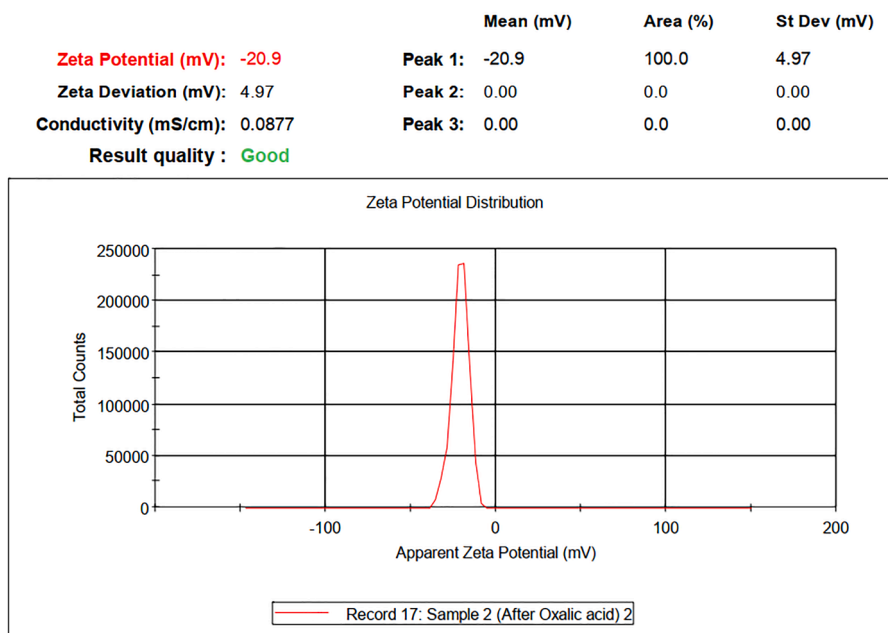


Fig. 4. Zeta Potential of the mycofabricated AgNPs.

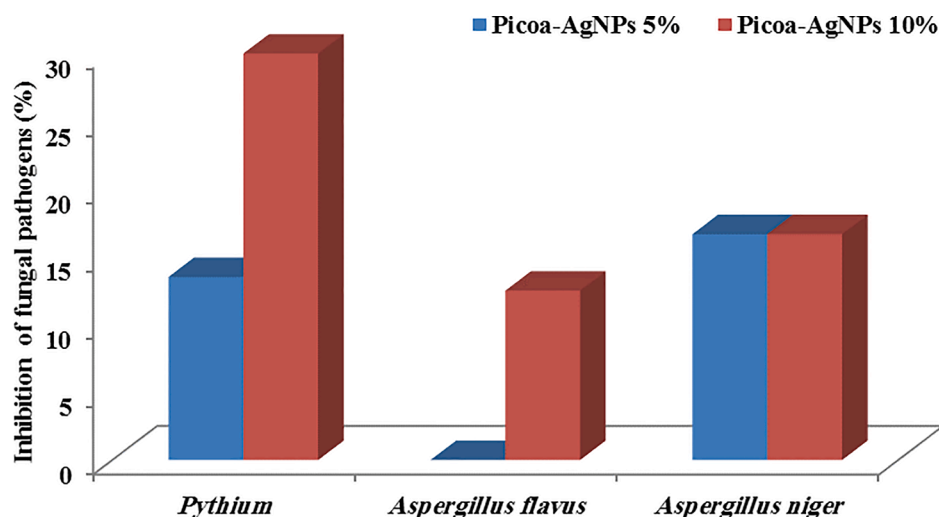


Fig. 5. Inhibition percentages (antifungal activity) of the Picoa-AgNPs against fungal pathogens. Legend: (Picoa-AgNPs 5%): 5% the used concentration of Picoa-AgNPs to inhibit three fungal pathogens, (Picoa-AgNPs 10%): 10% the used concentration of Picoa-AgNPs to inhibit three fungal pathogens.

(-20.9 mV); see Fig. 4.

Antifungal activity of the mycofabricated Picoa-AgNPs has been achieved on Potato Dextrose Agar at two concentrations, including 5% and 10%, separately. The antifungal activity has been done against three fungal pathogens, involving *Aspergillus flavus*, *Aspergillus niger*, and *Pythium* sp. The ascocarp extract of the Picoa truffle (the same concentration used in the synthesis of AgNPs) did not show any inhibitory effect against all pathogens. The inhibition percentages of the mycofabricated AgNPs from Picoa ascocarp extract were done as in Fig. 5. The higher inhibition percentage of Picoa-AgNPs was 30.81% against *Pythium* sp. at the concentration of 10%, while the concentration of 5% showed a low inhibitory effect (13.51%). The concentration of 5% and 10% exhibited a similar inhibitory effect reached 16.67% against *Aspergillus niger*. Moreover, the concentration of 10% showed an inhibitory effect reached 12.50% toward *Aspergillus flavus* pathogen, whereas 5% Picoa-AgNPs did not show any inhibitory effect against the last fungal pathogen. Generally, mushroom extracts have antifungal activity against many fungi

(Owaid et al., 2017). Mushroom-AgNPs are important to inhibit pathogens (Owaid, 2019a) includes bacteria and fungi (Owaid, 2020). These results agreed with the results of (Jaloot et al., 2020) reported that the mushroom *Inonotus hispidus*-AgNPs have antifungal activity against some fungal pathogens.

The role of the mycofabricated AgNPs is potent and remarkable against microbes compared to the truffle extract alone. Also, the large surface area of the mycofabricated AgNPs makes interactions of AgNPs with cellular membranes (Morones et al., 2005) and gives more surface contact with the pathogen's surface (Logeswari et al., 2015). AgNPs adhere and contact the cell membrane and wall of the bacterium and fungus. Hence some silver ions release and adhere to sulphur-containing proteins on cellular membranes (Brunner et al., 2006; Klasen, 2000). The interactions on microbes' cellular membranes lead to many structural formations and morphological changes on the microbial surfaces, including pits and pores. These changes (pores) lead to the release of microbes' components into extracellular fluids because of the osmotic

difference. While AgNPs across cellular membranes and interact with DNA and RNA then inhibit the proteins replication process inside the microbe (death of microbes) by suppressing enzymes (Brunner et al., 2006; Feng et al., 2000; Yamanaka et al., 2005).

The current work results agree with the finding of Owaid (2019a). However, AgNPs showed an inhibitory impact on some fungi like *Bipolaris sorokiniana* and *Colletotrichum* sp. (Lamsal et al., 2011). Besides, the AgNP decreases the production of mycotoxins in *A. niger* and *A. flavus* and reduces the cytotoxicity of molds. AgNPs also exhibited effectiveness on the produced organic acid from *A. niger* (Pietrzak et al., 2016). The toxicity of AgNPs due to the production of ROS (reactive oxygen species) or to the direct interaction and disruption of biomacromolecules (Brunner et al., 2006). Many researchers reported that the mycosynthesized AgNPs had antimicrobial efficacies (Owaid, 2019b). These results also agree with green AgNPs in the recent studies like *Ganoderma applanatum*-AgNPs (Jogaiah et al., 2019), *Dillenia indica*-AgNPs (Nayak et al., 2020), and *Trichoderma harzianum*-AgNPs (Konappa et al., 2021); they were applied as nanodrugs against various pathogenic bacteria.

4. Conclusion

A few studies have been performed on the effectiveness of green silver nanoparticles to prevent plant diseases. This study attempts to synthesize green silver-nanoparticles using a new reducing agent (*Picoa*, Pezizales) for plant protection. Visual and instrumental analyzes indicated the formation of silver nanoparticles. The higher inhibition percentage of *Picoa*-AgNPs was 30.81% against *Pythium* sp. The concentration of 5% exhibited an inhibitory effect reached 16.67% against *Aspergillus niger*. Hence, those mycofabricated AgNPs are important to prevent or inhibit some fungal plant pathogens. This study advice is to use *Picoa*-AgNPs in different applications and to mycosynthesize new metallic nanoparticles in future. These findings have shown a promising outlook for the use of *Picoa* (Pezizales) in the production of AgNPs for its use as antifungal nanodrug.

Declaration of Competing Interest

The authors declare that they have no known competing financial interests or personal relationships that could have appeared to influence the work reported in this paper.

Acknowledgement

This work was supported by the Ministry of Higher Education Malaysia (MOHE), FRGS Grant [203/PFIZIK/6711768], and the authors would also like to thank School of Physics, Universiti Sains Malaysia, for access to supporting facilities related to this research work.

References

- AbdelRahim, K., Mahmoud, S.Y., Ali, A.M., Almaary, K.S., Mustafa, A.-Z., Husseiny, S.M., 2017. Extracellular biosynthesis of silver nanoparticles using *Rhizopus stolonifer*. *Saudi J. Biol. Sci.* 24 (1), 208–216. <https://doi.org/10.1016/j.sjbs.2016.02.025>.
- Abdul-Hadi, S.Y., Owaid, M.N., Rabeea, M.A., Abdul Aziz, A., Jameel, M.S., 2020. Rapid mycosynthesis and characterization of phenols-capped crystal gold nanoparticles from *Ganoderma applanatum*. *Ganodermataceae. Biocatal. Agric. Biotechnol.* 27, 101683. <https://doi.org/10.1016/j.cbab.2020.101683>.
- Ahn, E.Y., Jin, H., Park, Y., 2019. Assessing the antioxidant, cytotoxic, apoptotic and wound healing properties of silver nanoparticles green-synthesized by plant extracts. *Mater. Sci. Eng. C* 101, 204–216. <https://doi.org/10.1016/j.msec.2019.03.095>.
- Al-Bahrani, R., Raman, J., Lakshmanan, H., Hassan, A.A., Sabaratnam, V., 2017. Green synthesis of silver nanoparticles using tree oyster mushroom *Pleurotus ostreatus* and its inhibitory activity against pathogenic bacteria. *Mater. Lett.* 186, 21–25. <https://doi.org/10.1016/j.matlet.2016.09.069>.
- Anand, K., Gengan, R.M., Phulukdaree, A., Chuturgoon, A., 2015. Agroforestry waste moringa oleifera petals mediated green synthesis of gold nanoparticles and their anti-cancer and catalytic activity. *J. Ind. Eng. Chem.* 21, 1105–1111. <https://doi.org/10.1016/j.jiec.2014.05.021>.

- Bawadekji, A., Abdelrazek, M., Mridha, M.A.U., Al Ali, M., 2016. Importance of *Picoa* spp. as desert truffles fungi. *J. Pure Appl. Microbiol.* 10, 297–304.
- Bhattarai, B., Zaker, Y., Bigioni, T.P., 2018. Green synthesis of gold and silver nanoparticles: Challenges and opportunities. *Curr. Opin. Green Sustain. Chem.* 12, 91–100. <https://doi.org/10.1016/j.cogsc.2018.06.007>.
- Brunner, T.J., Wick, P., Manser, P., Spohn, P., Grass, R.N., Limbach, L.K., Bruinink, A., Stark, W.J., 2006. In vitro cytotoxicity of oxide nanoparticles: Comparison to asbestos, silica, and the effect of particle solubility. *Environ. Sci. Technol.* 40, 4374–4381. <https://doi.org/10.1021/es052069i>.
- Chen, G., Zhang, S., Ran, C., Wang, L., Kan, J., 2016. Extraction, characterization and antioxidant activity of water-soluble polysaccharides from *Tuber huidongense*. *Int. J. Biol. Macromol.* 91, 431–442. <https://doi.org/10.1016/j.ijbiomac.2016.05.108>.
- Dheyab, M.A., Owaid, M.N., Rabeea, M.A., Aziz, A.A., Jameel, M.S., 2020. Mycosynthesis of gold nanoparticles by the Portabella mushroom extract, Agaricaceae, and their efficacy for decolorization of Azo dye. *Environ. Nanotechnol. Monit. Manage* 14, 100312. <https://doi.org/10.1016/j.enmm.2020.100312>.
- Eskandari-Nojehdehi, M., Jafarizadeh-Malmiri, H., Rahbar-Shahrouzi, J., 2018. Hydrothermal green synthesis of gold nanoparticles using mushroom (*Agaricus bisporus*) extract: Physico-chemical characteristics and antifungal activity studies. *Green Process Synth* 7, 38–47. <https://doi.org/10.1515/gps-2017-0004>.
- Eskandari-Nojehdehi, M., Jafarizadeh-Malmiri, H., Rahbar-Shahrouzi, J., 2016. Optimization of processing parameters in green synthesis of gold nanoparticles using microwave and edible mushroom (*Agaricus bisporus*) extract and evaluation of their antibacterial activity. *Nanotechnol. Rev.* 5, 537–548. <https://doi.org/10.1515/ntrev-2016-0064>.
- Feng, Q.L., Wu, J., Chen, G.Q., Cui, F.Z., Kim, T.N., Kim, J.O., 2000. A mechanistic study of the antibacterial effect of silver ions on *Escherichia coli* and *Staphylococcus aureus*. *J. Biomed. Mater. Res.* 52, 662–668. [https://doi.org/10.1002/1097-4636\(20001215\)52:4<662::AID-JBM10>3.0.CO;2-3](https://doi.org/10.1002/1097-4636(20001215)52:4<662::AID-JBM10>3.0.CO;2-3).
- Gherbawy, Y.A., Shalaby, I.M., El-Sadek, M.S.A., Elhariry, H.M., Abdelilah, B.A., 2013. The anti-fascioliasis properties of silver nanoparticles produced by *Trichoderma harzianum* and their improvement of the anti-fascioliasis drug Triclabendazole. *Int. J. Mol. Sci.* 14, 21887–21898. <https://doi.org/10.3390/ijms141121887>.
- Gopinath, V., Velusamy, P., 2013. Extracellular biosynthesis of silver nanoparticles using *Bacillus* sp. GP-23 and evaluation of their antifungal activity towards *Fusarium oxysporum*. *Spectrochim. Acta Part A Mol. Biomol. Spectrosc.* 106, 170–174. <https://doi.org/10.1016/j.saa.2012.12.087>.
- Gupta, N., Upadhyaya, C.P., Singh, A., Abd-El salam, K.A., Prasad, R., 2018. Applications of Silver Nanoparticles in Plant Protection 247–265. https://doi.org/10.1007/978-3-319-91161-8_9.
- Iravani, S., Korbekandi, H., Mirmohammadi, S.V., Zolfaghari, B., 2014. Synthesis of silver nanoparticles: chemical, physical and biological methods. *Res. Pharm. Sci.* 9, 385–406.
- Ismail, M., Prasad, R., Ibrahim, A.I.M., Ahmed, A.I.S., 2017. Modern Prospects of Nanotechnology in Plant Pathology, in: Prasad, R., Kumar, M., Kumar, V. (Eds.), *Nanotechnology*. Springer, Singapore, pp. 305–317. https://doi.org/10.1007/978-981-10-4573-8_15.
- Jaloot, A.S., Owaid, M.N., Naem, G.A., Muslim, R.F., 2020. Mycosynthesizing and characterizing silver nanoparticles from the mushroom *Inonotus hispidus* (Hymenochaetales), and their antibacterial and antifungal activities. *Environ. Nanotechnol. Monit. Manage.* 14, 100313. <https://doi.org/10.1016/j.enmm.2020.100313>.
- Jamali, S., Banihashemi, Z., 2013. Species-specific ITS primers for the identification of *Picoa juniperi* and *Picoa lefebvrei* and using nested-PCR for detection of *P. juniperi* in planta. *Mol. Biol. Rep.* 40 (10), 5701–5712. <https://doi.org/10.1007/s11033-013-2672-6>.
- Jogaiah, S., Kurjogi, M., Abdelrahman, M., Hanumanthappa, N., Tran, L.-S., 2019. *Ganoderma applanatum*-mediated green synthesis of silver nanoparticles: structural characterization, and in vitro and in vivo biomedical and agrochemical properties. *Arab. J. Chem.* 12 (7), 1108–1120. <https://doi.org/10.1016/j.arabjc.2017.12.002>.
- Khadri, H., Aldebasi, Y.H., Riazunnisa, K., 2017. Truffle mediated (*Terfezia clavayi*) synthesis of silver nanoparticles and its potential cytotoxicity in human breast cancer cells (MCF-7). *Afr. J. Biotechnol.* 16, 1278–1284. <https://doi.org/10.5897/AJB2017.16031>.
- Khandan Nasab, N., Sabouri, Z., Ghazal, S., Darroudi, M., 2020. Green-based synthesis of mixed-phase silver nanoparticles as an effective photocatalyst and investigation of their antibacterial properties. *J. Mol. Struct.* 1203, 127411. <https://doi.org/10.1016/j.molstruc.2019.127411>.
- Klasen, H.J., 2000. Historical review of the use of silver in the treatment of burns I. *Early uses. Burns* 26 (2), 117–130.
- Konappa, N., Udayashankar, A.C., Dhamodaran, N., Krishnamurthy, S., Jagannath, S., Uzma, F., Pradeep, C.K., De Britto, S., Chowdappa, S., Jogaiah, S., 2021. Ameliorated antibacterial and antioxidant properties by *trichoderma harzianum* mediated green synthesis of silver nanoparticles. *Biomolecules* 11 (4), 535. <https://doi.org/10.3390/biom11040535>.
- Lamsal, K., Kim, S.W., Jung, J.H., Kim, Y.S., Kim, K.S., Lee, Y.S., 2011. Application of silver nanoparticles for the control of *Colletotrichum* species in vitro and pepper anthracnose disease in field. *Mycobiology* 39 (3), 194–199. <https://doi.org/10.5941/MYCO.2011.39.3.194>.
- Logeswari, P., Silambarasan, S., Abraham, J., 2015. Synthesis of silver nanoparticles using plants extract and analysis of their antimicrobial property. *J. Saudi Chem. Soc.* 19 (3), 311–317. <https://doi.org/10.1016/j.jscs.2012.04.007>.
- Malik, P., Shankar, R., Malik, V., Sharma, N., Mukherjee, T.K., 2014. Green chemistry based benign routes for nanoparticle synthesis. *J. Nanoparticles* 2014, 1–14. <https://doi.org/10.1155/2014/302429>.

- Martínez-Tomé, M., Maggi, L., Jiménez-Monreal, A.M., Murcia, M.A., Marí, J.A.T., 2014. Nutritional and Antioxidant Properties of Terfezia and Picoa 261–273. https://doi.org/10.1007/978-3-642-40096-4_17.
- Morones, J., Elechiguerra, J., Camacho, A., Holt, K., Kouri, J., Ramírez, J., Yacaman, M., 2005. The bactericidal effect of silver nanoparticles. *Nanotechnology* 16, 2346–2353.
- Naeem, G.A., Jaloot, A.S., Owaid, M.N., Muslim, R.F., 2021. Green synthesis of gold nanoparticles from *Coprinus comatus*, agaricaceae, and the effect of ultraviolet irradiation on their characteristics. *Walailak J. Sci. Technol.* 18, 9396. <https://doi.org/10.48048/wjst.2021.9396>.
- Nayak, S., Bhat, M.P., Udayashankar, A.C., Lakshmeesha, T.R., Geetha, N., Jogaiah, S., 2020. Biosynthesis and characterization of *Dillenia indica*-mediated silver nanoparticles and their biological activity. *Appl Organomet Chem* 34, 1–9. <https://doi.org/10.1002/aoc.5567>.
- Owaid, M.N., 2017. Antagonistic role of hypha and cell-free culture filtrates of medicinal mushrooms to *Verticillium* sp. and *Pythium* sp. fungal pathogens. *Curr. Res. Environ. Appl. Mycol.* 7 (2), 94–102. <https://doi.org/10.5943/cream/10.5943/cream/210.5943/cream/7/2/6>.
- Owaid, M.N., 2018. Bioecology and uses of desert truffles (Pezizales) in the middle east. *Walailak J. Sci. Technol.* 15 (3), 179–188.
- Owaid, M.N., 2019a. Green synthesis of silver nanoparticles by *Pleurotus* (oyster mushroom) and their bioactivity: review. *Environ. Nanotechnol. Monit. Manage.* 12, 100256. <https://doi.org/10.1016/j.enmm.2019.100256>.
- Owaid, M.N., 2019c. Green synthesis of silver nanoparticles by *Pleurotus* (oyster mushroom) and their bioactivity: review. *Environ. Nanotechnol. Monit. Manage.* 12, 100256. <https://doi.org/10.1016/j.enmm.2019.100256>.
- Owaid, M.N., Raman, J., Lakshmanan, H., Al-Saeedi, S.S.S., Sabaratnam, V., Ali, I.A., 2015. Mycosynthesis of silver nanoparticles by *Pleurotus cornucopiae* var. *citrinopileatus* and its inhibitory effects against *Candida* sp. *Mater. Lett.* 153, 186–190. <https://doi.org/10.1016/j.matlet.2015.04.023>.
- Owaid, M.N., Al-Saeedi, S.S.S., Al-Assaffi, I.A.A., 2017. Antifungal activity of cultivated oyster mushrooms on various agro-wastes. *Summa Phytopathol.* 43 (1), 9–13. <https://doi.org/10.1590/0100-5405/2069>.
- Owaid, M.N., Muslim, R.F., Hamad, H.A., 2018. Mycosynthesis of silver nanoparticles using *Terminia* sp. Desert truffle, pezizaceae, and their antibacterial activity. *J. J. Biol. Sci.* 11, 401–405.
- Owaid, M.N., Rabeea, M.A., Abdul Aziz, A., Jameel, M.S., Dheyab, M.A., 2019. Mushroom-assisted synthesis of triangle gold nanoparticles using the aqueous extract of fresh *Lentinula edodes* (shiitake), *Omphalotaceae*. *Environ Nanotechnol. Monit. Manage.* 12, 100270. <https://doi.org/10.1016/j.enmm.2019.100270>.
- Owaid, M.N., Naeem, G.A., Muslim, R.F., Oleiwi, R.S., 2020. Synthesis, characterization and antitumor efficacy of silver nanoparticle from *Agaricus bisporus pileus*, *Basidiomycota*. *Walailak J. Sci. Technol.* 17 (2), 75–87.
- Owaid, M. N., 2019a. Silver nanoparticles as unique nano-drugs, in: Grumezescu, A.M., Grumezescu, V. (Eds.), *Materials for Biomedical Engineering: Bioactive Materials, Properties and Applications*. Elsevier, pp. 545–580.
- Owaid, M.N., 2020. Biomedical Applications of Nanoparticles Synthesized from Mushrooms, in: Patra, J., Fraceto, L., Das, G.C. (Eds.), *Green Nanoparticles. Nanotechnology in the Life Sciences*. Springer Nature Switzerland AG, pp. 289–303. https://doi.org/10.1007/978-3-030-39246-8_14.
- Pietrzak, K., Glińska, S., Gapińska, M., Ruman, T., Nowak, A., Aydin, E., Gutarowska, B., 2016. Silver nanoparticles: a mechanism of action on moulds. *Metallomics* 8 (12), 1294–1302. <https://doi.org/10.1039/C6MT00161K>.
- Purohit, J., Chattopadhyay, A., Singh, N.K., 2019. Green Synthesis of Microbial Nanoparticle: Approaches to Application, in: Prasad, R. (Ed.), *Microbial Nanobionics. Nanotechnology in the Life Sciences*. Springer, Cham., pp. 35–60. https://doi.org/10.1007/978-3-030-16534-5_3.
- Rabeea, M.A., Owaid, M.N., Aziz, A.A., Jameel, M.S., Dheyab, M.A., 2020. Mycosynthesis of gold nanoparticles using the extract of *Flammulina velutipes*, *Physalacriaceae*, and their efficacy for decolorization of methylene blue. *J. Environ. Chem. Eng.* 8 (3), 103841. <https://doi.org/10.1016/j.jece.2020.103841>.
- Roseline, T.A., Murugan, M., Sudhakar, M.P., Arunkumar, K., 2019. Nanopesticidal potential of silver nanocomposites synthesized from the aqueous extracts of red seaweeds. *Environ. Technol. Innov.* 13, 82–93. <https://doi.org/10.1016/j.eti.2018.10.005>.
- Shankar, S.S., Ahmad, A., Sastry, M., 2003. Geranium leaf assisted biosynthesis of silver nanoparticles. *Biotechnol. Prog.* 19 (6), 1627–1631. <https://doi.org/10.1021/bp034070w>.
- Srikar, S.K., Giri, D.D., Pal, D.B., Mishra, P.K., Upadhyay, S.N., 2016. Green synthesis of silver nanoparticles: a review. *Green Sustain. Chem.* 06 (01), 34–56. <https://doi.org/10.4236/gsc.2016.61004>.
- Suresh, A.K., Doktycz, M.J., Wang, W., Moon, J.W., Gu, B., Meyer III, H.M., Hensley, D. K., Retterer, S.T., Allison, D.P., Phelps, T.J., 2011. Monodispersed biocompatible Ag₂S nanoparticles: Facile extracellular bio-fabrication using the gamma-proteobacterium, *S. oneidensis*. Oak Ridge National Laboratory (ORNL); Center for Nanophase Materials Sciences; High Temperature Materials Laboratory.
- Wang, S., Marcone, M.F., 2011. The biochemistry and biological properties of the world's most expensive underground edible mushroom: Truffles. *Food Res. Int.* 44 (9), 2567–2581. <https://doi.org/10.1016/j.foodres.2011.06.008>.
- Yamanaka, M., Hara, K., Kudo, J., 2005. Bactericidal actions of a silver ion solution on *Escherichia coli*, studied by energy-filtering transmission electron microscopy and proteomic analysis. *Appl. Environ. Microbiol.* 71, 7589–7593. <https://doi.org/10.1128/AEM.71.11.7589>.